Journal of Power Technologies 104 (1) (2024) 86 -- 97

DC current oscillations reduction in MMC-HVDC system

Kamran Hafeez[1, ✉], Alex Van den Bossche[2]

[1]Department of Electrical and Computer Engineering, COMSATS University Park Road, Islamabad, Pakistan
[2]Department of Electrical Engineering, Metals, Mechanical constructions and systems, Ghent University 131, B9052, Gent Belgium
✉ voltagehigh@hotmail.com

Abstract

Modular multilevel converter (MMC) is a type of voltage source converter (VSC) that offers several advantages, permitting suitable technology in high voltage direct current (HVDC) transmission systems. In the conventional non-energy-based control method, current does not manage capacitor energies inside MMC modules and produces DC current oscillations. Whereas in energy-based control methods, oscillations in DC current are reduced as differential currents are controlled. In this paper a proportional resonant (PR) controller is designed to reduce oscillations in a DC-link of an HVDC system using non-energy-based control method. It reduces oscillations by injecting even order harmonics in MMC. The proposed method is tested on a symmetrical monopole point-to-point MMC-HVDC system using PSCAD simulation software. Furthermore, the proposed method is also compared with a conventional repetitive current (RC) controller using bode plots. Analytical and simulation results validate the proposed method.

Introduction

Voltage source converters (VSCs) utilize insulated gate bipolar transistors (IGBTs), whereas line commutated converters (LCCs) are based on silicon-controlled rectifiers (SCRs) as a switching device to control power. VSC is considered a better technology compared to LCC due to independent control of active and reactive power and reduced filtration requirements [1-2]. MMC is a type of VSC, suitable for high voltage direct-current (HVDC) based transmission systems. It offers the following key advantages; a) reduction in converters switching losses, b) scalable output voltage due to series connection of sub-modules (SMs) [3]. The dynamics of MMC include SM capacitor voltage fluctuations and circulating current that is generated among the phase units of a 3-phase MMC [4]. The MMC arm voltages can be generated using a direct modulation method [5], a closed loop [6], or open loop modulation method [7]. In direct modulation simple PWM is used to control converter output voltage and current. Circulating current is generated in direct modulation approach, as cyclic variations in capacitor voltages are not accounted. Conventionally CCSC is used to eliminate circulating current by converting this current into negative sequence double frequency rotating d-q reference frame more suitable for PI controllers referring as a non-energy-based approach.

However, this method results in oscillations in DC link currents [8-9]. In energy-based approach or compensated modulation, arms controllers are needed to make the system asymptotically stable [10]. Due to arm currents and circulating current interactions, traditional methods of linear stability analysis; linearization, Eigen value analysis and state space modeling cannot be applied directly to MMC [11]. In open loop compensated modulation arm voltages are estimated by measuring output current and DC link voltage without needing additional control loops for its stability [12]. However, stability is highly dependent on accurate information of circuit parameters. Analysis of MMC in non-energy- based control is also discussed using direct modulation but analytical equations are difficult to solve due to time varying model of MMC [13]. A repetitive current (RC) controller is developed for the stable operation of MMC without considering the relationship between state variables as energy functions [14]. Energy controllers are developed to manage capacitor energies by controlling differential currents, involving several control loops [15]. Different methods are also proposed in literature to control differential currents without removing oscillations from DC side currents [16-18]. Multiple proportional-resonant (PR) controllers and plug-in- repetitive controllers are used to eliminate even order harmonics from the differential currents to manage capacitor energies [19-20]. Due to cascaded loops and multiple- controllers involved, these methods are difficult to implement. The relationship between energy stored in MMC and DC voltage is reported in [21]. In energy-based control, several control loops are needed to stabilize a system, whereas in non-energy-based control method the system is balanced but oscillations are reported in DC currents in HVDC system [22]. Therefore, in this paper a PR controller is designed to reduce DC current oscillations in HVDC system using conventional non – energy-based control approach.

To the best of author's knowledge, the key contribution of this paper can be described as:

1) In non-energy-based control, output dc currents remain uncontrolled, and second harmonic component of the i_{diff} differential current is removed using a CCSC.

2) DC-side currents are not directly controlled in non-energy-based MMCs method that results in over-currents or oscillations.

3) In a conventional non-energy-based control 2nd and 4th harmonics are injected to reduce oscillations in the DC link currents.

4) Unlike [19], a simple PR controller is designed to track arm currents with the addition of even order harmonics in it.

5) Unlike [20], a PI controller is proposed for the output current control

and a simple PR controller is designed to control i_{diff} instead of conventional plug-in-RC controller.

6) The proposed control system is compared with a conventional non–energy control using CCSC to verify it.

MMC-HVDC Modeling

3-Phase MMC Configuration

The 3-phase circuit diagram of MMC consists of identical sub-modules (SMs) connected in series as shown in Figure 1. The SMs are used to build a half-bridge circuit topology for an MMC. Each SM is made of a capacitor and two insulated-gate bipolar transistors (IGBTs) working as switches T_1 and T_2 connected in series. The cell output voltage (V_{SM}) is equal to the capacitor voltage (T_1 on state) or zeros (T_1 off state) and is regulated by the controller. The SMs switching states are controlled so that at any instant N SMs out of $2N$ SMs are on (N_{up} in the upper arm and $N_{low} = N - N_{up}$ in the lower arm) in each phase. Each arm of 3-phase MMC has N series connected SMs linked to an inductor L_{arm} used to limit fault currents [23].

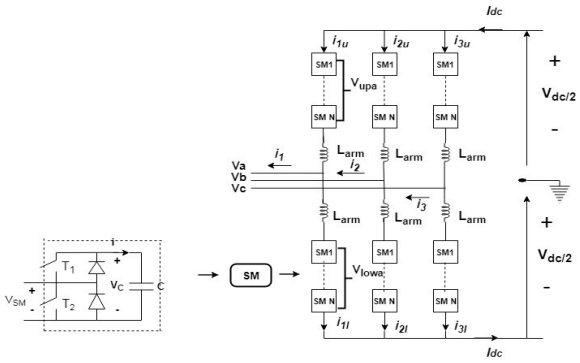

Figure 1: 3-Phase MMC

The upper and lower currents in each arm of 3-phase MMC are equal to half of the phase current i_1 one third of DC current i_{dc} and the circulating current i_{cir} . Where i_{1u} and i_{1l} are the arm currents and i_{cir} is the loop current.

$$i_{1u} = \frac{i_1}{2} + \frac{i_{dc}}{3} + i_{cir} \quad (1)$$

$$i_{1l} = -\frac{i_1}{2} + \frac{i_{dc}}{3} + i_{cir} \quad (2)$$

The differential current i_{diff} from Equation (2) consists of two current components:

$$i_{diff} = \frac{i_{1u} + i_{1l}}{2} \quad (3)$$

$$V_{diff} = \frac{V_{dc}}{2} - \frac{V_{upa} + V_{lowa}}{2} \quad (4)$$

$$V_o = \frac{V_{dc}}{2} - V_g - L_1 \frac{di_1}{dt} - R_1 i_1 \quad (5)$$

Since $i_1 = i_{1u} - i_{1l}$, state space model of MMC is given as; $X = [i_1\ i_{diff}\ i_{1u}\ V_{up\,a}^{\Sigma}\ V_{low\,a}^{\Sigma}]^T$ and system inputs $U = [V_o^*\ V_{diff}^*]^T$, the outputs are selected as $Y = [i_1\ i_{diff}]^T$.The MMC output voltage V_o in phase a using Fig.1 can be described as:

$$V_o = \sum_{n=1}^{N} S_n V_c \quad (6)$$

Where V_c is the SM capacitor voltage and S_n is given as:

$$S_n = \begin{bmatrix} 1, & \text{if n cell is inserted} \\ 0, & \text{if nth cell is bypassed} \end{bmatrix}$$

Switching signal (s) corresponds to the MMC arm voltages based on insertion index. It has two types a) uncompensated b) compensated modulation as given in equation (7) and (8).

$$n_u = \frac{e^*{}_a - V^*{}_{diff}}{V_{dc}} \quad (7)$$

$$n_l = \frac{e_a{}^* - V^*{}_{diff}}{V^{\Sigma}{}_{upa}} \quad (8)$$

Where n_u and n_l represents upper arm and lower arm insertion indices. In direct modulation method or non-energy-based control, arm capacitor oscillations are not accounted for and CCSC controller is required since V_{diff} is voltage remains uncontrolled. Whereas in compensated modulation arm capacitor voltages are measured or estimated. It includes additional control loops for stability [24]. Therefore, in this paper direct modulation method is implemented.

MMC-HVDC System

A two terminal symmetrical monopole MMC-HVDC system is shown in Figure 2(a). Each MMC working as a controllable DC voltage source is linked to an AC system using a 3-phase transformer (T_1) , (T_2). A master-slave method is used, in which MMC-1 (rectifier) controls the DC voltage and MMC-2 (Inverter) controls the active power. The reactive power can be regulated independently at each side of AC system. Grid connected MMC at each terminal is shown in Figure 2(b) and 2 (c).

The proposed control system shown in Figure 2(b) is compared with plug- in RC controller as given in [20] is shown in Figure 2(c). The outer power controller calculates current references for the inner current control system. It is implemented in a $d-q$ rotating reference frame by connecting each MMC to a grid represented by a 3- phase voltage source. Park's and Clarke's transformation are used to convert I_{abc} currents into I_d and I_q axis current components described as:

$$\begin{bmatrix} I_d(t) \\ I_q(t) \\ I_o(t) \end{bmatrix} = \frac{2}{3}\begin{bmatrix} \sin(\omega_o t) & \sin\left(\omega_o t - \frac{2\pi}{3}\right) & \sin\left(\omega_o t + \frac{2\pi}{3}\right) \\ \cos(\omega_o t) & \cos\left(\omega_o t - \frac{2\pi}{3}\right) & \cos\left(\omega_o t + \frac{2\pi}{3}\right) \\ \frac{1}{2} & \frac{1}{2} & \frac{1}{2} \end{bmatrix} \cdot \begin{bmatrix} I_{(a)}(t) \\ I_{(b)}(t) \\ I_{(c)}(t) \end{bmatrix} \quad (9)$$

The inner controller generates reference voltage $e_a = \frac{V_{upa} - V_{lowa}}{2}$ to control output current i_1 .Where ωt is the voltage phase angle to be extracted by the Phase Locked Loop (PLL) at the point of common coupling (PCC) i.e. θ. The control of active (P) and reactive power (Q) based on current references I_d and I_q can be expressed as [25]:

$$P = \frac{3}{2} V_d i_d + V_q i_q \quad (10)$$

$$Q = -\frac{3}{2} V_d i_q + V_q i_d \quad (11)$$

Where V_d and V_q shows the voltage values at the PCC in d-q axis, respectively. Since PLL is synchronized to grid voltage, the q-axis component of voltage becomes zero. The I_d and I_q can be regulated by changing its reference values.

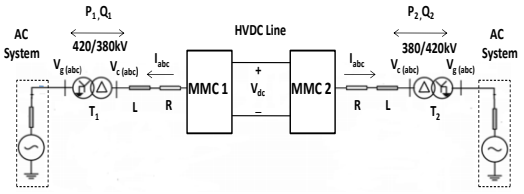

(a)

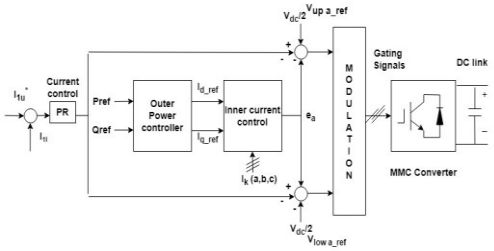

(b)

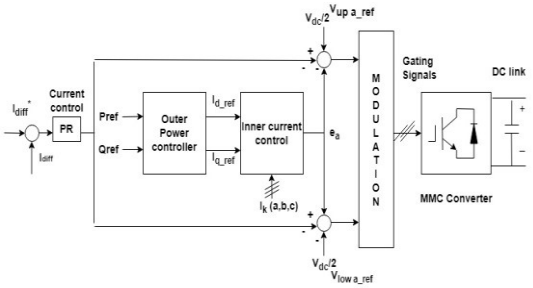

(c)

Figure 2: MMC-HVDC system a) Two terminal MMC b) Grid connected MMC proposed c) Grid connected MMC conventional, plug-in –RC controller

Current Control System Design

The control loops for both the systems as shown in Figure 2 are in simplified form given in Figure 3. The reference output current i_1^* is calculated using active and reactive power commands based on vector current control strategy in this paper using equations (10-11). Unlike [20] PI controller is used for the output current control instead of PR controller as shown in Figure 3(a). The inner current control is similar for both the proposed and conventional systems. The i_{diff}^* current reference is calculated by sub-module capacitor voltage control in a conventional system. Then i_{diff} current is regulated by a repetitive controller (RC) cascaded with a PI to eliminate multiple harmonics as proposed in [20] is shown in Figure 3(b). However, in the proposed system a simple nonideal-PR controller is designed to regulate arm currents references i_{1u}^* and i_{1l}^* with addition of harmonics in it to reduce i_{diff} as shown in Figure 3(c).

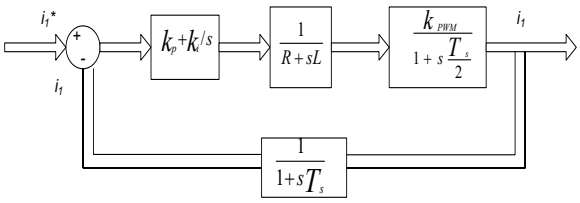

(a)

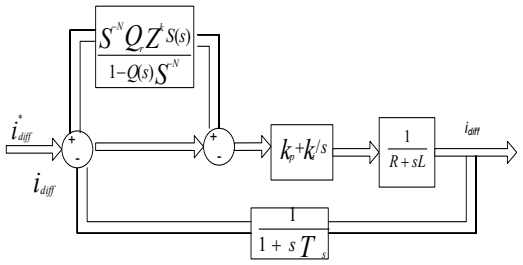

(b)

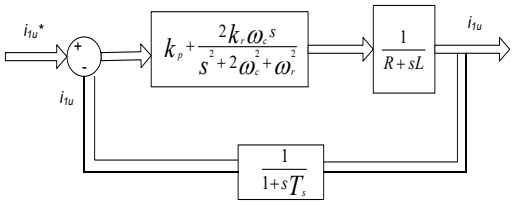

(c)

Figure 3: Simplified control loops a) output current control b) differential current control conventional plug-in-RC controller) (c) proposed control system

The plant transfer function is given in s domain in equation (12) and its discrete form using bilinear transformation (Tustin) method is given in equation (13):

$$G(s) = \frac{1}{R + sL} \tag{12}$$

$$G(s) = \frac{T_s(1 + Z^{-1})}{RT_s + L + (RT_s - L)Z^{-1}} \tag{13}$$

Where T_s is sampling interval and z is the frequency domain operator.

The open loop transfer functions of all the three loops in s domain; a) output current control b) differential current control plug-in-RC controller; c) Proposed control shown in Figure (3) can be described as:

$$G_{tf_1} = \left(k_p + \frac{k_i}{s}\right).\frac{k_{pwm}}{1 + s\frac{T_s}{2}}.\frac{1}{1 + sT_s}.\frac{1}{R + sL} \tag{14}$$

$$G_{tf2} = \left(\frac{S^{-N}Q_rZ^kS(s)}{1-Q(s)S^{-N}}\right).\left(k_p + \frac{k_i}{s}\right) \ .\frac{1}{1+sT_s}.\ \frac{1}{R+sL} \tag{15}$$

$$G_{tf3} = \left(k_p + \frac{2k_r\omega_c s}{s^2 + 2\omega_c^2 + \omega_r^2}\right).\frac{1}{1 + sT_s}.\frac{1}{R + sL} \tag{16}$$

Where k_{pwm} is the gain of PWM which is equal to the ratio of DC voltage and line-to-line AC voltage of the converter. Normally PWM is selected as one half of the sampling time. The Q_r is the gain of RC controller and $S(s)$represents a low pass filter and $Q(s)$ is a filter constant [26].

Using parameters in Table -II, following transfer functions are derived from equations (14-16):

$$G_{tf1} = \left(k_p + \frac{k_i}{s}\right).\frac{1.19}{0.000000015s^3 + 0.8} \tag{17}$$

$$G_{tf2} = \left(\frac{S^{-N}Q_rz^kS(s)}{1-Q(s)S^{-N}}\right).\left(k_p + \frac{k_i}{s}\right).\frac{1}{0.0000156s^2+0.799} \tag{18}$$

$$G_{tf3} = \left(k_p + \frac{2k_r\omega_c s}{s^2+2\omega_c^2+\omega_r^2}\right).\frac{1}{0.0000156s^2+0.799} \tag{19}$$

Three control systems a) PI controller b) RC controller c) PR controller transfer functions in discrete forms using bi-linear transformation can be given as:

$$G_{tf1}(z) = k_p + k_iT_s\frac{1}{z - 1} \tag{20}$$

$$G_{tf2}(z) = \frac{z^{-N}Q_rz^kS(z)}{1 - Q(z)Z^{-N}} \tag{21}$$

$$G_{tf3}(z) = k_p + \frac{z-1}{2k_rT_s\omega_c\frac{}{z^2+(T_s^2.\omega_r^2-2+2\omega_cT_s).z+1-2\omega_cT_s}} \tag{22}$$

The expression for $S(z)$ in equation (21) can be defined as:

$$S(s) = \frac{\omega_n^2}{s^2 + 2\xi\omega_n s + \omega_n^2} \tag{23}$$

Were ω_n is angular corner frequency and ξ is damping ratio. The corner frequency is selected $f_n = 96$ Hz and $\xi = 0.707$ .The equation (23) is discretized with switching frequency $f_s = 960$ Hz given as:

$$\frac{0.06397z^2 + 0.1279z + 0.06397}{z^2 - 1.168z + 0.4242} \tag{24}$$

Since z^k is a phase delay, N is the number of samples in one fundamental cycle. Plug-in-RC controller is

designed to eliminate 2nd harmonic in a differential current by considering; $\frac{f_s}{2\times f} = N = 9$ samples.Where f_s is the sampling frequency and f represents the fundamental frequency. The controller parameters are given in Table 1.

Table 1 Controller parameters

Symbol	Description	Values
K_p	PR controller gain	1
kr	PR controller resonant gain	10
ω_r	PR controller cut-off frequency	12 rad/s
Q_r	RC controller gain	2
k	phase delay RC controller	6
Q_z	Damping ratio RC controller	0.707
Q_s	Filter constant RC controller	0.96
K_p	Proportional gain PI-plug in RC	1.733
K_i	Integral gain PI-plug in RC	133.47

The frequency plot of output current control loop, G_{tf1} is shown in Figure 4. Phase- margin and gain- margin is around 56º and 5 dB based on PI values k_p=7.024 and k_i=0.158. The closed loop system is stable [27].

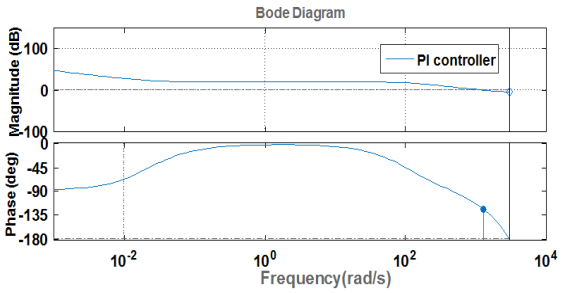

Figure 4: Bode plot output current control loop

The bode plots of i_{diff} current loop plug-in- RC controller and proposed control system, G_{tf2} and G_{tf3} shown in Figure 5 (a) and 5(b).

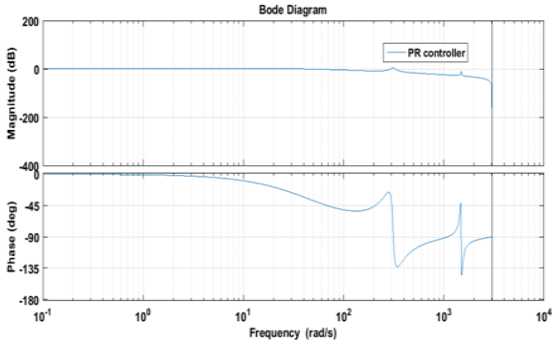

(a)

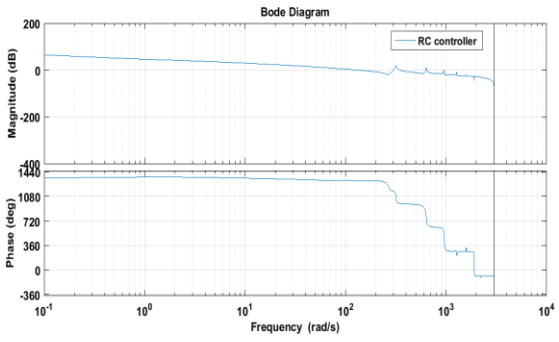

(b)

Figure 5: Bode plots a) Proposed control system b) Plug-in- RC controller

The PR compensator is designed at resonant frequency $\omega_r = 628$ rad/s (100Hz) and $\omega_r = 1884$ rad/s (200Hz) to track sinusoidal arm currents as evident

from the bode plots. The Phase-margin is around 53º, which shows the closed loop system is stable.

The plug-in-RC controller is designed to eliminate 2nd harmonic (100Hz) from the differential current as shown in Figure 5(b). The phase margin is around 51º, that shows the closed loop system is stable. However, as reported in [28], the harmonic tracking ability of conventional plug-in-RC controller reduces, if f_{break} or corner frequency > 2nd order frequency, thus making its design complex. Therefore, this method is not further implemented. The tracking performance of proposed controlled is given in Figure (6). The step response to plant is shown in Figure 6(a). The plant output is required to track reference signal. The tracking output of proposed PR controller follows the reference signal with no overshoot and oscillations with almost zero tracking error as shown in Figure 6(b).

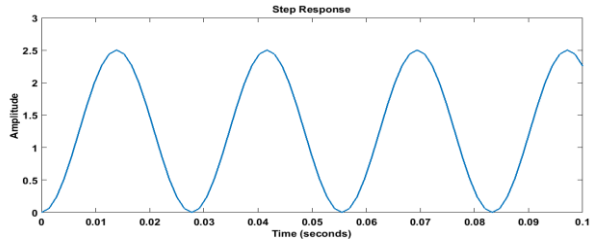

(a)

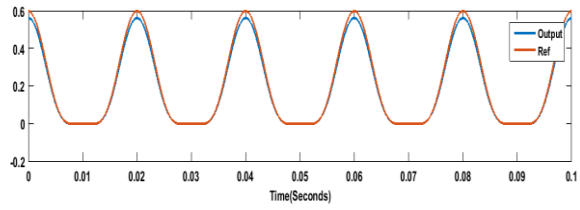

(b)

Figure 6: a) Step response b) Tracking output of reference signal

The direct modulation method using two voltage references generated by $d-q$ control system can be expressed as [29]:

$$V_{upa_{ref}} = \frac{V_{dc}}{2}[1 - mcos(\omega_0 t)] - e_a - V_{diff} \quad (25)$$

$$V_{lowa_{ref}} = \frac{V_{dc}}{2}[1 + mcos(\omega_o t)] - e_a - V_{diff} \quad (26)$$

The term m shows the modulation index (amplitude) and ω_o is angular frequency. The circulating current i_{diff} is not controlled in direct modulation approach in this paper.

i_{diff} is reduced by adding 2nd and 4th harmonics in each arm currents of an MMC [30]. The analytical results of i_{diff} using equation (3) for the conventional and proposed methods are given in Figure 7.

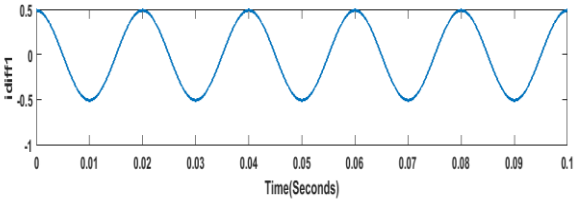

(a)

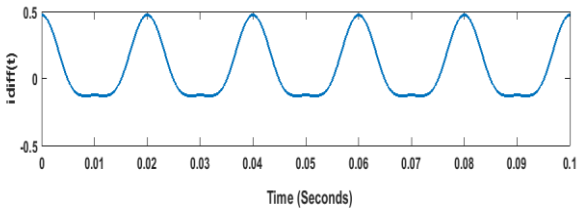

(b)

Figure 7: i_diff current a) conventional method b) proposed method

SIMULATION RESULTS

The proposed and conventional model is tested on MMC-HVDC system model shown in Figure 3 using PSCAD software. Thevenin equivalent model reported in [31] is implemented to develop a symmetrical point-to-point MMC-HVDC system in this paper. To balance SMs capacitor voltages, phase shifted PWM and sorting algorithms are used [32].The capacitor voltage balancing is achieved by using nearest level modulation method (NLM,) as discussed in [33].The active and reactive power at two terminals are controlled at their reference values P=960MW and Q=40 MVAr as shown in Figure 8(a) and Figure 8(b). DC bus voltage is controlled around its reference value of

640 kV. The MMC grid side 3-phase line to line output voltage is shown in Figure 8(c). The parameters of MMC- HVDC system are given in Table 2.

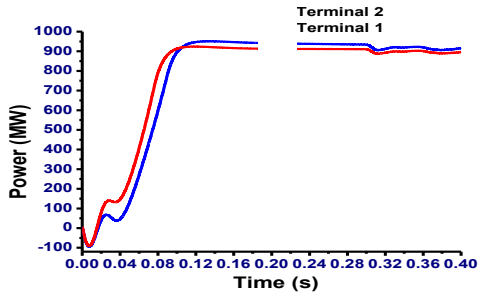

(a)

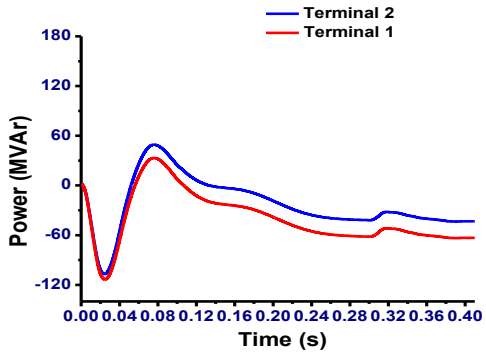

(b)

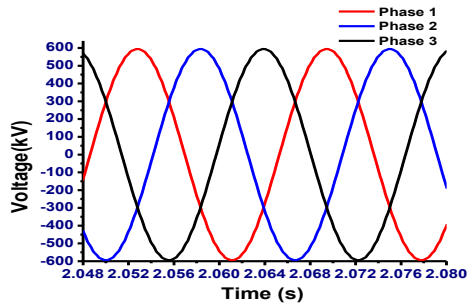

(c)

Figure 8: Results of (a) P1, P2 at T1 and T2; (b) Q1, Q2 at T1 and T2 (c) AC side converter voltage

The conventional non-energy-based control using CCSC method with DC side current oscillations are shown in Fig 9(a). Since DC-side currents are not directly controlled in MMCs that results in over-currents or oscillations [34-35]. The suppression of circulating currents does not eliminate capacitor voltage fluctuations completely in MMC [36]. Whereas in proposed control method DC side current oscillations are shown in Fig.9 (b). Since i_{diff} current is eliminated using a conventional method. In the proposed method i_{diff} is not eliminated but it reduces the oscillations in the DC side currents by injecting 2nd and 4th harmonics in the arm currents.

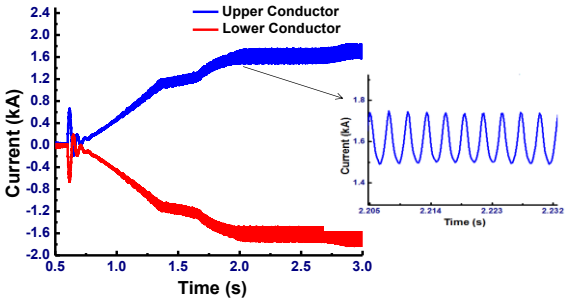

(a)

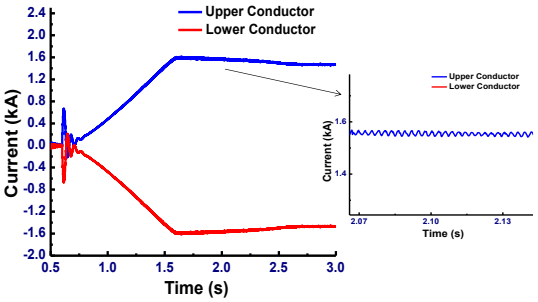

(b)

Figure 9: Results of (a) DC side current conventional (b) DC side current proposed

The conventional non-energy-based control, upper arm currents in MMC is shown in Figure 10(a) whereas in proposed control, upper arm currents is shown in Figure 10(b). The MMC arm current is injected with 2nd and 4th harmonics.

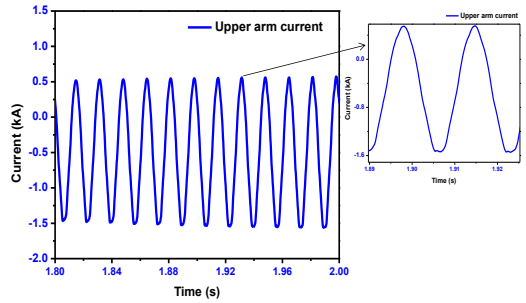

(a)

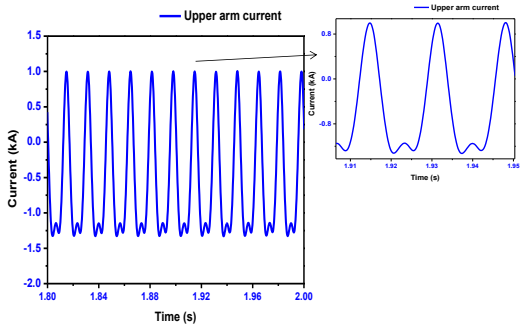

(b)

Figure 10: Results of (a) upper arm currents conventional (b) upper arm currents proposed

The conventional $d-q$ based output currents are shown in Figure 11(a). Whereas in proposed output currents is shown in Figure 11(b).

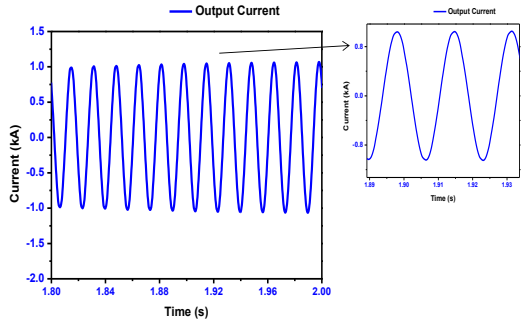

(a)

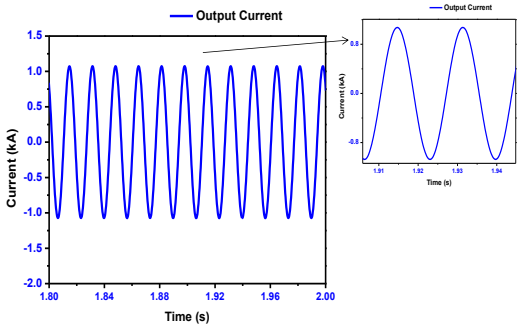

(b)

Figure 11: Results of (a) Output currents conventional (b) Output currents proposed

The rms harmonic magnitude of output current from Figure 11 (b) is shown in Figure 12. The output currents have the highest rms value of the fundamental frequency.

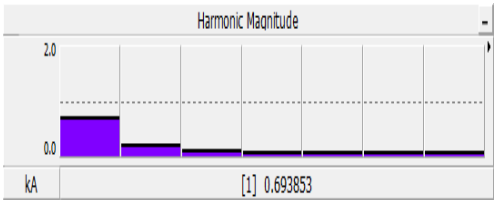

Figure 12: Results of (a) harmonic magnitude

The MMC HVDC system parameters are given in Table 2 below:

Table 2 HVDC system parameters

Parameter	Value
Apparent power (S)	1000MVA
Active power (P)	960MW
Converter side AC voltage	380kV
DC side voltage	±320 kV
DC side current	1.5kA
Transformer connection	Y/△
Cell capacitor	2800 µF
Arm inductance	76 mH
Transformer inductance	15 mH
Arm resistance	0.8 Ω
DC Line (two conductors)	15 km
Ac side Power Factor ($Cos\emptyset_L$)	0.96
Angular frequency (ω)	314 rad/s
Sampling frequency	960 Hz
Sampling interval (Ts)	0.00104 s

CONCLUSION

A conventional non-energy-based control with 2nd and 4th harmonics in the arm currents is proposed in this paper. It helped to reduce the DC current oscillations without using a differential current control method in MMC-HVDC system. A simple PR control system is designed to track the arm currents of MMC using bode plots. This system is also compared against conventional plug-in-RC controller that has complex design due to interactions between PI and RC controllers. Furthermore, the proposed system is tested on MMC based HVDC system using PSCAD software and also verified analytically. In the next paper other differential current control methods will be compared with the proposed method.

Declarations

Ethical Approval

Not Applicable

Competing interests

The authors have no relevant financial or non-financial interests to disclose.

Authors' contributions

Dr. Kamran Hafeez provided the initial concept, written up with simulation results and finally overviewed by Prof. Alex Van den Bossche.

Funding

The author(s) received no specific funding for this work.

Availability of data and materials

The data are all contained within the manuscript and fully available without restriction.

References

1. Kamran Hafeez, Ahmed Bilal Awan, " To Investigate Environmental effects of HVDC versus HVAC Transmission Systems' J. Basic. Appl. Sci. Res., 3(8)840-843, 2013.
2. N. Flourentzou, V. Agelidis, and G. Demetriades, "VSC based HVDC power transmission systems: an overview," Power Electronics, IEEE Transactions on, vol. 24, no. 3, pp. 592-602, 2009.
3. S. Rohner, S. Bernet, M. Hiller, and R. Sommer, "Modulation, losses, and semiconductor requirements of modular multilevel converters," IEEE Trans. Ind. Electron., vol. 57, no. 8, pp. 2633-2642, Aug. 2010.

4. L. Harnefors, A. Antonopoulos, S. Norrga, L. Angquist, and H. Nee," Dynamic analysis of modular multilevel converters," IEEE Trans. Ind. Electron., vol. 60, no. 7, pp. 2526-2537, Jul. 2013.
A. Antonopoulos, L. Ängquist, and H.-P. Nee, "On dynamics and voltage control of the modular multilevel converter," in Proc. 13th European Conf. Power Electronics and Applications EPE '09, 2009, pp. 1-10.
5. L. Harnefors, S. Norrga, A. Antonopoulos, and H.-P. Nee, "Dynamic modeling of modular multilevel converters," in Proc. 2011-14th European Conf. Power Electronics and Applications (EPE 2011), 2011, pp. 1-10.
6. L. Ängquist, A. Antonopoulos, D. Siemaszko, K. Ilves, M. Vasiladiotis, and H.-P. Nee, "Open-loop control of modular multilevel converters using estimation of stored energy," IEEE Trans. Ind. Appl., vol. 47, no. 6, pp. 2516-2524, Nov.-Dec. 2011.
7. Antonopoulos,K.; A.; Norrga, S.; Nee, H.P. Steady-State Analysis of Interaction between Harmonic Components of Arm and Line Quantities of Modular Multilevel Converters. IEEE T. Power Electr.2012, 27, 57-68.
8. T. Li, A. Gole, and C. Zhao, "Stability of a modular multilevel converter based hvdc system considering dc side connection," IET Conference Proceedings, pp.1-6, January 2016.
9. K. Sharifabadi, L. Harnefors, H. P. Nee, S. Norrga, and R. Teodorescu, Design, Control and Application of Modular Multilevel Converters for HVDC Transmission Systems. Hoboken, NJ, USA: Wiley,2016.
A. Jamshidifar and D. Jovcic, "Small signal dynamic dq model of modular multilevel converter for system studies," Power Delivery, IEEE Transactions on, vol. 31, pp. 191-199, February 2016.
10. L. Harnefors, A. Antonopoulos, K. Ilves, and H. Nee, "Global asymptotic stability of current-controlled modular multilevel converters," IEEE Trans. Power Electron., vol. 30, no. 1, pp. 249-258, Jan. 2015.
11. N. R. Chaudhuri, R. Oliveira, and Y. Yazdani, "Stability analysis of vector-controlled modular multilevel converters in linear time-periodic framework," IEEE Trans. Power Electron., vol. 31, no. 7, pp. 5255-5269, Jul. 2016.
12. Kolluri, S., Gorla, N.B.Y., Sapkota, R., et al. 'A repetitive and Lyapunov function-based control approach for improved steady state and dynamic performance of modular multilevel converters'. 43rd Annual Conf. of the IEEE Industrial Electronics Society, Beijing, China, 29 October-1 November 2017, pp. 687-692.
13. G. Bergna et al., "An energy-based controller for HVDC modular multilevel converter in decoupled double synchronous reference frame for voltage oscillation reduction," IEEE Trans. Ind. Electron., vol. 60, no. 6, pp. 2360-2371, Jun. 2013
14. Picas,R.; Pou, J.; Ceballos,S.; Zaragoza,J.; Konstantinou,G.; Agelidis , "Optimal injection of harmonics in circulating currents of modular multilevel converters for capacitor voltage ripple minimization'. In Proceedings of the IEEE ECCE Asia Down under, Melbourne, VIC, Australia; pp. 318-324.2013.
15. J. Wang, X. Han, H. Ma, and Z. Bai, "Analysis and injection control of circulating current for modular multilevel converters," IEEE Trans. Ind.Electron., vol. 66, no. 3, pp. 2280-2290, Mar. 2019.
16. Q. Tu, Z. Xu, and L. Xu, "Reduced switching-frequency modulation and circulating current suppression for modular multilevel converters," IEEETrans. Power Del., vol. 26, no. 3, pp. 2009-2017, Jul. 2011.
17. S. Li, X. Wang, Z. Yao, T. Li, and Z. Peng, "Circulating current suppressing strategy for MMC-HVDC based on non-ideal proportional resonant controllers under unbalanced grid conditions," IEEE Trans. Power Electron. Vol. 30, no. 1, pp. 387-397, Jan. 2015.
18. L. He, K. Zhang, J. Xiong, and S. Fan, "A repetitive control scheme for harmonic suppression of circulating current in modular multilevel converters," IEEE Trans. Power Electron., vol. 30, no. 1, pp. 471-481, Jan. 2015.

19. S. Samimi, F. Gruson, P. Delarue, F. Colas, M. M. Belhaouane, and X. Guillaud, "MMC stored energy participation to the dc bus voltage control in an HVDC link," IEEE Trans. Power Del., vol. 31, no. 4, pp. 1710-1718, Aug. 2016.
20. E.Prieto-Araujo, A. Junyent-Ferré, C. Collados-Rodríguez, G. Clariana-Colet, and O. Gomis-Bellmunt, "Control design of Modular Multilevel Converters in normal and AC fault conditions for HVDC grids," Electr. Power Syst. Res., vol. 152, pp. 424-437,2017.
21. Hagiwara, M.; Akagi, H, " PWM control and experiment of modular multilevel converters. In Proceedings of the IEEE Power Electronics Specialists Conference, Rhodes, Greece; pp. 154-16, 2008.
22. Angquist, L.; Antonopoulos, A.; Siemaszko, D.; Ilves, K.; Vasiladiotis, M.; Nee, H.P. Inner control of Modular Multilevel Converters-An approach using open-loop estimation of stored energy. In Proceedings of the Power Electronics Conference (IPEC), International, Sapporo, Japan, 21-24 June 2010; pp. 1579-1585
23. Shuhui, L., Haskew, T.A., Ling, X, "Control of HVDC light system using conventional and direct current vector control approaches'', IEEE Trans. Power Electron., 2010, vol. 25, pp. 3106-3118. 2010.
24. M. S. Ali, L. Wang, H. Alquhayz, O. U. Rehman and G. Chen, "Performance Improvement of Three-Phase Boost Power Factor Correction Rectifier Through Combined Parameters Optimization of Proportional-Integral and Repetitive Controller," in IEEE Access, vol. 9, pp. 58893-58909, 2021,
25. Hafeez, K., Khan, S.A., Van Den Bossche, A. et al. Capacitor voltage ripple reduction in MMC-HVDC system using flat bottom current method. Electr Eng ,2021.
26. B. Li, D. Xu, and D. Xu, "Circulating Current Harmonics Suppression for Modular Multilevel Converters Based on Repetitive Control," Journal of Power Electronics, vol. 14, no. 6, pp. 1100-1108, Nov. 2014.
27. Siemaszko, D.; Antonopoulos, A.; Ilves, K.; Vasiladiotis, M.; Angquist, L.; Nee, H.P. Evaluation of control and modulation methods for modular multilevel converters. In Proceedings of the 2010 International Power Electronics Conference (IPEC), Sapporo, Japan, 21-24 June 2010; pp. 746-753.
28. Kamran Hafeez, Shahid A. Khan, Alex Van den Bossche, Qadeer UL Hasan,' Circulating Current Reduction in MMC-HVDC System Using Average Model'. Appl. Sci., 9, 1383.2019.
29. U. N. Gnanarathna, A. M. Gole, and R. P. Jayasinghe, "Efficient modeling of modular multilevel HVDC converters (MMC) on electromagnetic transient simulation programs," IEEE Trans. Power Del., vol. 26, no. 1, pp. 316-324, Jan. 2011.
30. Z. Zhao, K. Li, Y. Jiang, S. Lu and L. Yuan, "Overview on reliability of modular multilevel cascade converters," in Chinese Journal of Electrical Engineering, vol. 1, no. 1, pp. 37-49, Dec. 2015
31. Q. Tu and Z. Xu, "Impact of sampling frequency on harmonic distortion for modular multilevel converter," IEEE Trans. Power Del.,vol. 26, no. 1, pp. 298-306, Jan. 2011.
32. Freytes J, Bergna G, Suul JA, D'Arco S, Gruson F, Colas F, et al. Improving small signal stability of an mmc with ccsc by control of the internally stored energy. IEEE Trans Power Del Feb. 2018;33(1):429-39.
33. J. Freytes, G. Bergna, J. Suul, S. D'Arco, H. Saad, and X. Guillaud, "Small-signal model analysis of droop-controlled modular multilevel converters with circulating current suppressing controller," in Proc. 13th IET Int. Conf. AC DC Power Transm., Feb. 2017, pp. 16-24.
34. Fujin Deng, Yongqing Lü, Chengkai Liu. 'Overview on Submodule Topologies, Modeling, Modulation, Control Schemes, Fault Diagnosis, and Tolerant Control Strategies of Modular Multilevel Converters'' in Chinese Journal of Electrical Engineering, vol. 6, no. 1, pp. 1-21, Dec. 2020